yield in both phases is strongly dependent on the temperature used, here $T = 145$ MeV. In QGP, we took $m_{\rm c} = 1.3$ GeV. The phase space of a HG includes all known charmed mesons and baryons, with abundances of light quarks controlled by $\mu_{\rm b} = 210$ MeV and $\mu_{\rm s} = 0$.

Although, by choosing a slightly higher value of T, we can easily increase the equilibrium yield of charm in a HG to the QGP level [133], this does not eliminate the effect of canonical suppression of production of charm if chemical equilibrium is assumed for charm in the elementary interactions. We are simply so deep in the 'quadratic' domain of the yield, see Eq. (11.60), that playing with parameters changes nothing, since we are constrained in Pb–Pb interactions by experiment to have a yield of charm of less than one pair.

It is natural to argue that the very heavy charm quarks are not in chemical equilibrium, and that their production has to be studied in kinetic theory of collision processes of partons. However, this means that there is no twenty-first-century Maxwell's demon with control of charm, and, of course, also not of strangeness. The production and enhancement of charm and strangeness in heavy-ion collisions is in our opinion a kinetic phenomenon. To study it, we should explore a wide range of collision volume and energy. The objective is to determine boundaries of the high, possibly QGP-generated, yields.

12 Hagedorn gas

12.1 The experimental hadronic mass spectrum

One of the most striking features of hadronic interactions, which was discovered by Hagedorn [140], is the growth of the hadronic mass spectrum with the hadron mass. With the 4627 different hadronic states we have used in the study of properties of HG in section 11.1 [136], it is reasonable to evaluate the mass spectrum of hadronic states $\rho(m)$, defined as the number of states in the mass interval $(m,\ m + dm)$. We represent each particle by a Gaussian, and obtain $\rho(m)$ by summing the contributions of individual hadronic particles:

$$\rho(m) = \sum_{m^*=m_\pi,m_\rho,\dots} \frac{g_{m^*}}{\sqrt{2\pi}\sigma_{m^*}} \exp\left(-\frac{(m-m^*)^2}{2\sigma^2_{m^*}}\right). \tag{12.1}$$

Here, g_{m^*} is the degeneracy of the hadron of mass m^* including, in particular, spin and isospin degeneracy, and $\sigma = \Gamma/2$, $\Gamma = \mathcal{O}(200)$ MeV being the width of the resonance. The pion, with $m_\pi \simeq \sigma$ is a special case, and is set aside in such smoothing of the mass spectrum. Downward modification of its mass has a great impact on properties of HG and is thus not allowed.

https://doi.org/10.1017/9781009290753.017 Published online by Cambridge University Press

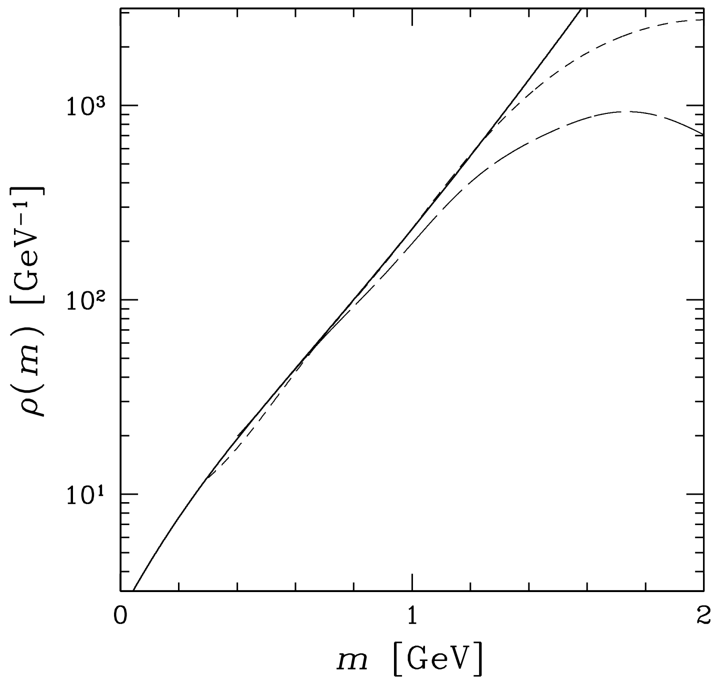

Fig. 12.1. Dashed lines are the smoothed hadronic mass spectrum. The solid line represents the fit Eq. (12.2) with $k = -3$, $m_0 = 0.66$ GeV, and $T_0 = 0.158$ GeV. Long-dashed line: 1411 states of 1967. Short-dashed line: 4627 states of 1996.

We compare the logarithm of the resulting smoothed mass spectrum for the hadronic particles known in 1967 (long-dashed line) with that for those known in 1996 (short-dashed line) in Fig. 12.1. We see that, in the 20 years following Hagedorn's last study of the phenomenon, the newly classified hadron resonances have improved the exponential behavior. We refer to a hadronic gas with an exponential mass spectrum as a Hagedorn gas. The solid line in Fig. 12.1 represents a fit using the empirical shape

$$\rho(m) \approx c(m_0^2 + m^2)^{k/2} \exp(m/T_0) \tag{12.2}$$

with $k = -3$. This value is preferred in the statistical-bootstrap model, section 12.2. However, many other values of k fit the mass spectrum well. The inverse slope T_0 and the preexponential power k are correlated in a fit of the mass-spectrum data and we present, in table 12.1, the results for several choices of k. We shall show that the value of k determines the behavior of the thermodynamic quantities of a gas of hadrons when $T \to T_0$ and its value is of some relevance.

https://doi.org/10.1017/9781009290753.017 Published online by Cambridge University Press

Table 12.1. Fitted parameters of Eq. (12.2) for given k

k	c	m_0	T_0
−2.5	0.83479	0.6346	0.16536
−3.0	0.69885	0.66068	0.15760
−3.5	0.58627	0.68006	0.15055
−4.0	0.49266	0.69512	0.14411
−5.0	0.34968	0.71738	0.13279
−6.0	0.24601	0.73668	0.12341
−7.0	0.17978	0.74585	0.11489

The mass spectra for fermions $\rho_{\rm F}(m)$ and bosons $\rho_{\rm B}(m)$ can differ, and, using these two functions, the generalization of Eq. (10.62) reads

$$\ln \mathcal{Z}_{\rm HG} = \frac{\beta^{-3}V}{2\pi^2}\sum_{n=1}^{\infty}\rho_n(m)\frac{1}{n^4}(n\beta m)^2K_2(n\beta m)\,, \tag{12.3}$$

where

$$\rho_n(m) \equiv \rho_{\rm B}(m) - (-1)^n\rho_{\rm F}(m)\,, \tag{12.4}$$

The Boltzmann approximation amounts to keeping in Eq. (12.3) the term with $n=1$, in which case

$$\rho(m) \equiv \rho_1(m) = \rho_{\rm B}(m) + \rho_{\rm F}(m). \tag{12.5}$$

To understand how the parameter k influences the behavior of the Hagedorn gas, we now introduce the asymptotic form Eq. (10.45) with the first term only, and consider the (classical, 'cl') Boltzmann limit,

$$\ln \mathcal{Z}_{\rm HG}^{\rm cl} = cV\left(\frac{T_0}{2\pi}\right)^{3/2}\int_{M_0}^{\infty} m^{k+3/2}e^{(m/T_0-m/T)}\,dm + D(T,M_0), \tag{12.6}$$

where $M_0 > m_0$ is a mass above which the asymptotic form of K_2 holds, and where $D(T,M_0)$ is finite. Because of the exponential factor, the integral is divergent for $T > T_0$, and the partition function is singular at T_0 for a range of k.

The pressure and the energy density for $T \to T_0$ are

$$P(T) \to \begin{cases} \left(\dfrac{1}{T}-\dfrac{1}{T_0}\right)^{-(k+5/2)}, & \text{for} \quad k > -\frac{5}{2}, \\ \ln\left(\dfrac{1}{T}-\dfrac{1}{T_0}\right), & \text{for} \quad k = -\frac{5}{2}, \\ \text{constant}, & \text{for} \quad k < -\frac{5}{2}; \end{cases} \tag{12.7}$$

https://doi.org/10.1017/9781009290753.017 Published online by Cambridge University Press

and

$$\epsilon \to \begin{cases} \left(\dfrac{1}{T}-\dfrac{1}{T_0}\right)^{-(k+7/2)}, & \text{for} \quad k>-\frac{7}{2}, \\ \ln\left(\dfrac{1}{T}-\dfrac{1}{T_0}\right), & \text{for} \quad k=-\frac{7}{2}, \\ \text{constant}, & \text{for} \quad k<-\frac{7}{2}. \end{cases} \tag{12.8}$$

The energy density goes to infinity for $k \geq -\frac{7}{2}$, when $T \to T_0$, and in this range falls the result of the statistical-bootstrap model with point hadrons, Eq. (12.35). Therefore T_0 appears as a limiting temperature for such a hadronic system [140].

Interestingly, the partition function and its derivatives may be singular at $T = T_0$ even when the volume of the system is finite, unlike the more conventional situation, with a true singularity expected only if the volume is infinite. However what is actually needed is an infinite number of participating particles, which in the conventional situation can occur only for $V \to \infty$. In relativistic statistical physics, particles are produced, and, for an exponential mass spectrum, an infinite number of particles arises already in a finite volume, for a sufficiently singular value of k and point-like hadrons, and $T \to T_0$. When hadrons of finite volume are considered, we find in section 12.3 that the energy density remains finite at $T = T_0$, independently of the value of the mass power k in the hadronic mass spectrum Eq. (12.2).

The reader will wonder whether the seemingly small difference between the exponential mass spectrum, and the so-far-known hadron mass spectrum, seen in Fig. 12.1 for $m > 1.5$ GeV, matters. We now compare the energy and pressure of HG evaluated using individual hadrons, thin lines in Fig. 12.2 (see also Fig. 11.1), with the results obtained using the analytical mass spectrum defined by Eq. (12.2), with parameters given in table 12.1. The vertical dotted line shows the limiting temperature for $k = -3$. Comparing the thick lines (exponential mass spectrum) with the results including known hadrons only (thin lines), we see in Fig. 12.2 significant differences both for ϵ/T^4 (a factor of four for $k = -3$) and P/T^4 (a factor of two for $k = -3$) in the physically relevant domain $T \simeq 150$ MeV. The various thick lines correspond to values of k listed in table 12.1 and can be assigned by noting at which value of temperature T_0 the singular behavior arises.

One would be tempted to conclude that, without full knowledge of the hadronic spectrum, we cannot use individual hadrons in the study of the properties of the HG, and hence evaluation of the total multiplicity of hadronic particles, as, e.g., is required in order to obtain Fig. 9.8 on page 169. There is, however, another effect, which counterbalances the

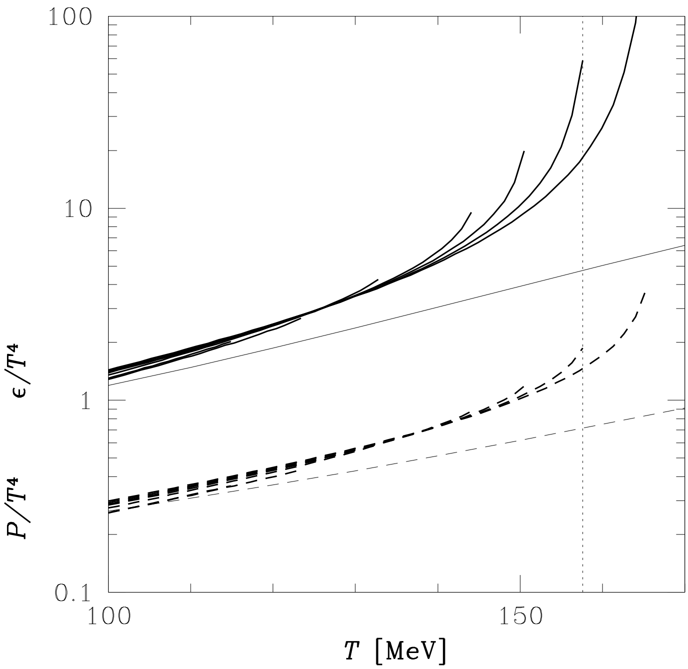

Fig. 12.2. The energy density ϵ/T^4 (solid lines) and pressure P/T^4 (dashed lines) (on a logarithmic scale) for a hadronic gas with a smoothed exponential mass spectrum, with values of $k = -2.5$ (the most divergent thick line) to $k = -7$ in steps of 0.5. The thin lines were obtained by using the currently known experimental mass spectrum. All fugacities γ and $\lambda = 1$.

effect of missing hadron resonances. When the finite size of a hadron is introduced, e.g., according to Eq. (11.1), significant decreases in magnitude of energy density, pressure, and number of particles at a given temperature ensue. For the value $\mathcal{B}^{1/4} = 190\,\mathrm{MeV}$, corresponding to $4\mathcal{B} = 0.68$ GeV fm^{-3}, a value we introduce to reproduce lattice QCD results in section 16.2, we show in Fig. 12.3 that there is practical agreement between the exponential mass-spectrum properties with finite-volume correction (thick lines) and the point hadron gas evaluated using known hadrons (long-dashed thin line for ϵ/T^4 and dotted thin line for P/T^4). Considering that the population of very massive resonances is not going to rise to full chemical equilibrium in nuclear collisions, along with the uncertainties in the finite-volume correction, (e.g., choice of $\mathcal{B}$) the remaining 15%–20% difference between the resonance gas with finite-volume correction and the point gas of known hadrons is not physically relevant. On the other hand, this clearly is the level of precision (theoretical systematic error) of the current computation of abundances of hadrons using

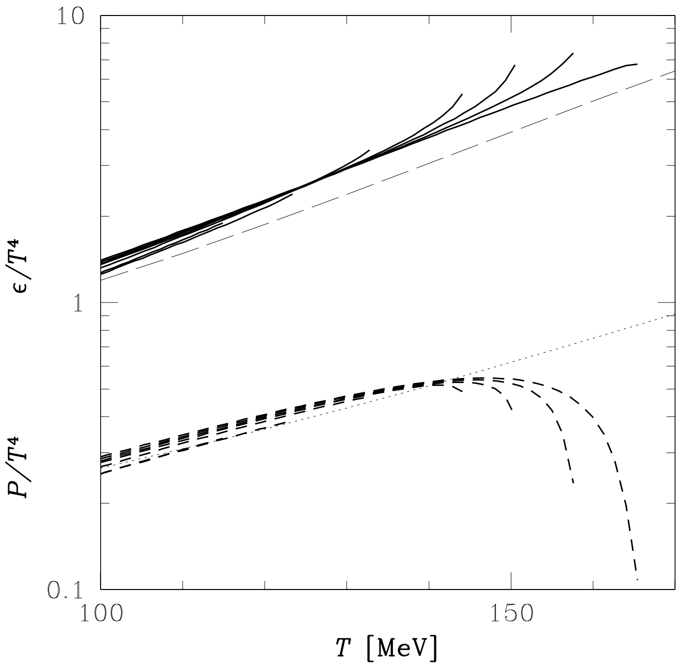

Fig. 12.3. The same as Fig. 12.2 but thick lines now show the gas of hadrons with an exponential mass spectrum including the finite-volume correction with $\mathcal{B} = (190\,\mathrm{MeV})^4$.

the known hadron spectrum. Most of this remaining systematic error disappears when hadron-abundance ratios are evaluated.

A cross check of the validity of the energy density and pressure obtained either by summing the physically known spectrum of point hadrons, or by employing the exponentially extrapolated spectrum of finitely sized hadrons is obtained by comparing them with lattice-gauge results. Results presented in section 15.5, in Fig. 15.3, show that, at the critical temperature, $\epsilon/T_{\rm c}^4 \simeq 6.5$. On comparing this with results shown in Fig. 12.3, we see that this result is consistent with the exponentially extrapolated results for $-3.5 \le k \le -2.5$ corrected for finite hadron volume, with 150 MeV $\lesssim T_{\rm c} \lesssim$ 165 MeV, the center of the range of lattice simulations. Using only the known point hadrons, a slightly larger value of $T_{\rm c} \simeq 171$ MeV is found. Comparison of pressure, shown in Fig. 12.3, with the lattice result in Fig. 16.2 is more difficult but clearly the results are also in qualitative agreement.

We have learned that the use in the field of heavy-ion collisions of a gas of point hadrons is justified because the contributions of probably still unknown hadronic resonances and the excluded-volume effect approximately cancel out. These remarks apply to all values of k we considered,

https://doi.org/10.1017/9781009290753.017 Published online by Cambridge University Press

though clearly the values $k = -3.5, -3$, and -2.5 are privileged by the comparison with lattice-gauge-theory results, and the value $k = -3$ is also central to the statistical-bootstrap model. We will now address this theoretical framework which leads to the exponential mass spectrum. We stress that our measure of singularity k refers in this book always to the point-particle theory; consideration of the finite hadronic volume removes the singular behavior of the hadronic energy density.

12.2 The hadronic bootstrap

To study interacting hadrons in a volume V, we first consider the N-particle level density $\sigma_N(E, V)$, a generalization of Eq. (4.37). σ_N generates the N-particle partition function,

$$Z_N(\beta, V) = \int \sigma_N(E, V) e^{-\beta E} dE. \tag{12.9}$$

For the non-interacting case, the number of states σ_N of N particles is obtained by carrying out the momentum integration Eq. (4.36) for each particle, keeping the total momentum $\vec{P} = 0$ and the energy E fixed. We divide by $N!$ for indistinguishable particles of degeneracy g and obtain

$$\sigma_N(E, V) = \frac{g^N V^N}{(2\pi)^{3N} N!} \prod_{i=1}^{N} \int \delta\Big(\sum_{i=1}^{N} \varepsilon_i - E\Big) \delta^3\Big(\sum_{i=1}^{N} \vec{p}_i\Big) d^3 p_i, \tag{12.10}$$

where the single-particle energy Eq. (4.31) is $\varepsilon_i = \sqrt{p_i^2 + m^2}$.

If an interaction between these particles is such that they form a bound state with mass m^* and nothing else happens, then the level density of this new system, including the effect of interaction, would be described as a mixture of ideal gases, one of mass m and the other of mass m^*. The logarithm of the partition function of such a system is additive, and the interaction in the gas of the mass m is accounted for by allowing for the presence of the second gas of mass m^*.

Beth and Uhlenbeck [64] formulated this argument more precisely for the case in which the interaction leads to the formation of a resonance in a scattering process, e.g.,

$$\pi + \mathrm{N} \to \Delta \to \pi + \mathrm{N}.$$

In such a case, the ℓth partial wave will be at large distances,

$$\psi_\ell(r, p) \sim \frac{1}{pr} \sin\Big(pr - \frac{\ell\pi}{2} + \eta_\ell(p)\Big), \tag{12.11}$$

where $\eta_\ell(p)$ is the phase shift due to scattering.

https://doi.org/10.1017/9781009290753.017 Published online by Cambridge University Press

To simplify, we argue in a manner similar to the study of the level density above Eq. (4.37). We consider a large sphere of radius R. The wave function Eq. (12.11) should vanish at $r = R$:

$$pR - \frac{\ell\pi}{2} + \eta_\ell(p) = n_\ell \pi\,; \qquad n_\ell = 0,\, 1,\, 2, \ldots. \tag{12.12}$$

n_ℓ labels the allowed two-body spherical momentum states $\{p_0,\, p_1,\, \ldots\}$. The density of states of angular momentum ℓ at p is $\Delta n_\ell/\Delta p$ and

$$\frac{dn_\ell}{dp} = \frac{R}{\pi} + \frac{1}{\pi}\frac{d}{dp}\eta_\ell(p). \tag{12.13}$$

Without interaction, $\eta_\ell(p) \equiv 0$, and we recognize that the interaction changes the two-particle density of states by $(1/\pi)\, d\eta_\ell/dp$.

We recall that the presence of a resonance leads to a rapid phase shift by π over the width of the resonance. In what follows, we shall assume that hadronic resonances are narrow, thus

$$\frac{1}{\pi}\frac{d\eta_\ell(p')}{dp} \approx \sum_{*} \delta(p' - p^*). \tag{12.14}$$

Such a δ-function appearing in the density of states Eq. (12.13) is exactly equivalent to the introduction of additional particles with masses m^*, which can be obtained from the masses of scattered particles and the relative momentum of the resonance p^*.

Consider now the probability for an N-body final state in a collision,

$$\begin{aligned} P(E,N) &= \int |\langle f|S|i\rangle|^2 \delta\Big(E - \sum_{i=1}^{N} E_i\Big)\delta^3\Big(\sum_{i=1}^{N}\vec{p}_i\Big)\prod_{i=1}^{n} d^3p_i \\ &\equiv \int |S|^2\, dR_N\Big(E, m_1, m_2, \ldots, m_N\Big), \end{aligned} \tag{12.15}$$

where the second expression introduces a short-hand notation for the N-particle phase-space volume element dR_N. Note that, in the Fermi model [121], the S-matrix element $|\langle f|S|i\rangle|^2$ is taken to be constant. Now we use Eq. (12.13) with Eq. (12.14) assuming that there is just one resonance. Then

$$\begin{aligned} P(E,N) &= \int |S'|^2\, dR_N\Big(E, m_1, m_2, \ldots, m_N\Big) \\ &\quad + \int |S'|^2\, dR_{N-1}\Big(E, m^*, m_3, \ldots, m_N\Big). \end{aligned} \tag{12.16}$$

The first term comes from R/π in Eq. (12.13) and the second term from $(1/\pi)\, d\eta_\ell(p')/dp'$ as given by Eq. (12.14) when there is a resonance in the

ℓth partial wave. We write S' instead of S to indicate that the part of the interaction responsible for the existence of a resonance between particles 1 and 2 is eliminated from S [63].

This manipulation was first done by Belenkij [63], but, until the work of Hagedorn [140], it was not pushed to its full consequences, involving many resonances, and the observation that the hadronic interactions are completely dominated by resonances. In that case, one can continue the process that led from Eq. (12.15) to Eq. (12.16) and the final hadronic state produced in any interaction is described by the sum over all possible N-particle phase spaces involving all possible hadronic states characterized by the mass spectrum $\rho(m)$, Eqs. (12.1) and (12.2).

Knowledge of all phase shifts in all channels, including, $2, 3, \ldots, n$-body phase shifts, is equivalent to the definition of the full S-matrix. If hadronic resonances characterize the phase shifts, then one can say that knowledge of the resonance spectrum determines the physics considered, or in reverse, hadronic interactions manifest themselves solely by the formation of resonances.

Can $\rho(m)$ be estimated in some way from the hypothesis that resonances dominate strong interactions? We follow the arguments of Hagedorn of 1965 [140], the statistical-bootstrap hypothesis. Consider the partition function given by Eq. (12.3) in the classical Boltzmann limit:

$$Z^{\text{cl}}_{\text{HG}}(V,T) = \exp\left[\frac{VT}{2\pi^2}\int_0^\infty \rho(m) m^2 K_2\!\left(\frac{m}{T}\right) dm\right]. \tag{12.17}$$

This equation expresses the partition function of the hadronic system of volume V at temperature T in terms of the hadrons whose hadronic mass spectrum is $\rho(m)$. Since we are looking for the asymptotic form of $\rho(m)$, we can replace the Bessel function $K_2(m/T)$ in Eq. (12.17) by its asymptotic form, Eq. (10.45), to obtain

$$Z^{\text{cl}}_{\text{HG}}(V,T) \simeq \exp\left[\int_0^\infty \left(\frac{mT}{2\pi}\right)^{3/2} \rho(m) e^{-m/T}\, dm\right]. \tag{12.18}$$

The Boltzmann factor $e^{-m/T}$ in the partition function shows that, with rising temperature, the contribution of resonance states of higher masses becomes more and more important.

On the other hand, the partition function of the same hadronic system can be written in terms of the density of all single-particle hadronic levels $\sigma_1(E,V)$:

$$Z^{\text{cl}}_{\text{HG}}(V,T) = \exp\left(\sum_i e^{-E_i/T}\right) = \exp\left(\int_0^\infty \sigma_1(E,V) e^{-E/T} dE\right). \tag{12.19}$$

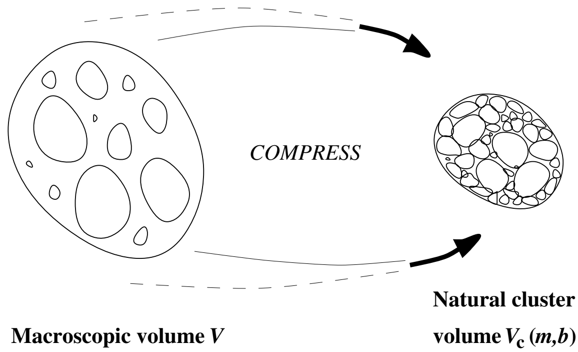

Fig. 12.4. The statistical-bootstrap idea: a system compressed to the 'natural cluster volume' becomes itself a cluster (consisting of clusters (consisting of . . .)).

The partition function $Z^{\rm cl}_{\rm HG}(V,T)$ for the same hadronic system is expressed in two different ways, once in term of the mass spectrum of its *constituents* and once in term of the density of states of the system as a *whole*. The physical meanings of $\sigma(E,V)$ and of $\rho(m)$ must be clearly understood:

- $\sigma_1(E,V)dE$ is the number of states between E and $E+dE$ of an interacting system enclosed in an externally given volume V; and
- $\rho(m)\,dm$ is the number of different hadronic resonance states between m and $m+dm$ of an interacting system confined to its 'natural volume' $V_{\rm c}$, i.e., to the volume resulting from the forces keeping interacting hadrons together as resonances.

Now, if we could compress a macroscopic hadron system to that small volume which would be the natural volume $V_{\rm c}(E)$ corresponding to the energy E, it would itself become another hadron, just one among the infinite number counted by the mass spectrum $\rho(m)$. This bootstrap idea is represented in Fig. 12.4. This hypothesis implies that Eq. (12.10) can now be written as an equation for the hadronic mass spectrum, which we cast into relativistically covariant form, akin to the form we discuss below, Eq. (12.63), including finite volume and baryon number

$$\boxed{\begin{aligned}\mathcal{H}\rho(p^2) &= \mathcal{H}\delta_0(m^2-m_{\rm in}^2)\\ &\quad+\sum_{N=2}^{\infty}\frac{1}{N!}\int\delta^4\!\left(p-\sum_{i=1}^{N}p_i\right)\prod_{i=2}^{N}\mathcal{H}\rho(p_i^2)d^4p_i,\end{aligned}} \tag{12.20}$$

where $\mathcal{H}\propto V_{\rm c}$, and we have separated out the first 'input' term. As before, $\delta_0(p^2-m^2)=\Theta(p_0)\delta(p^2-m^2)$. Eq. (12.20) is the statistical-bootstrap equation for the hadronic mass spectrum. There are two input constants entering, namely $\mathcal{H}$ and the mass $m_{\rm in}$ in the single-particle term. All other hadrons are clusters in their respective volumes, generated by this single particle of mass $m_{\rm in}$.

Interestingly, a semi-analytical solution of Eq. (12.20) is available. We consider the relativistic four-dimensional Laplace transform of Eq. (12.20),

$$\int e^{-\beta\cdot p}\,\mathcal{H}\rho(p^2)\,d^4p = \varphi(\beta) + \sum_{N=2}^{\infty}\frac{1}{N!} \times \prod_{i=1}^{N}\int e^{-\beta\cdot p_i}\,\mathcal{H}\rho(p_i^2)\,d^4p_i, \tag{12.21}$$

where there appears on the right-hand side, because of the δ-function in Eq. (12.20), the product of N identical independent integrals. Defining φ and G by

$$\varphi(\beta) = \int e^{-\beta\cdot p}\,\mathcal{H}\delta_0(p^2 - m_{\rm in}^2)d^4p = \mathcal{H}2\pi m_{\rm in}^2\frac{K_1(\beta m_{\rm in})}{\beta m_{\rm in}}, \tag{12.22}$$

and

$$G = \int e^{-\beta\cdot p}\,\mathcal{H}\rho(p^2)\,d^4p \tag{12.23}$$

we see that Eq. (12.21) becomes,

$$G(\varphi) = \varphi + e^{G(\varphi)} - G(\varphi) - 1, \tag{12.24}$$

or,

$$\varphi = 2G(\varphi) - e^{G(\varphi)} + 1. \tag{12.25}$$

Given the Laplace transform of the hadronic mass spectrum $G(\varphi)$, Eq. (12.23), one can use an inverse Laplace transform to obtain $\rho(m)$ or, at least, to determine its asymptotic behavior, in which we are interested. How one can proceed to solve Eq. (12.25) is shown in Fig. 12.5. We draw on the left in Fig. 12.5(a) the curve $G(\varphi)$ and then invert it, here 'graphically' on the right in Fig. 12.5(b). We see that this solution branch satisfies

$$G(\varphi) \le \ln 2 = G_0, \tag{12.26}$$

and increases as a function of

$$\varphi \le \varphi_0 = \ln(4/e), \tag{12.27}$$

up to the point where it has a root singularity. We have for $\varphi \to \varphi_0$:

$$G(\varphi) \approx G_0 \pm \text{constant} \times \sqrt{\varphi_0 - \varphi} + \cdots. \tag{12.28}$$

https://doi.org/10.1017/9781009290753.017 Published online by Cambridge University Press

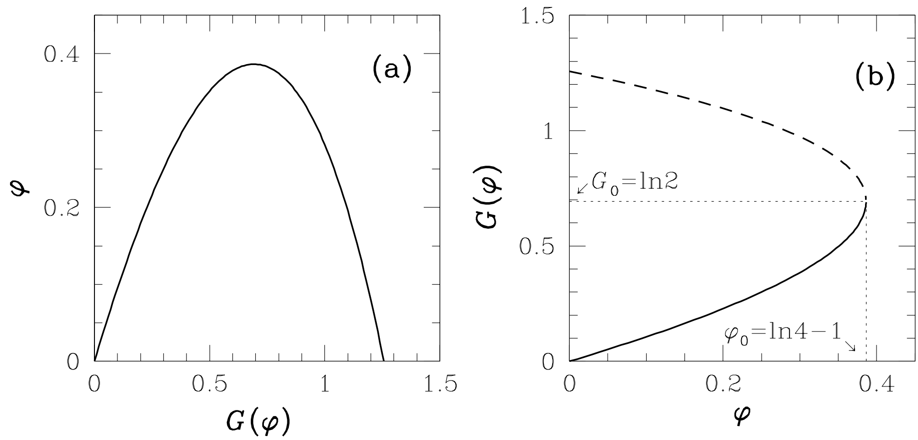

Fig. 12.5. (a) $G(\varphi)$ according to Eq. (12.25); (b) the graphical solution of Eq. (12.24).

For $\varphi \geq \varphi_0$, $G(\varphi)$ becomes complex and there are non-physical branches of the solution.

It is the square-root singularity of $G(\varphi)$ which determines that the mass power k of the hadronic mass spectrum $cm^k \exp(m/T_0)$ is $k = -3$. We recall that φ is actually itself defined in terms of β by Eq. (12.22), and it is monotonically decreasing with β: there is a minimum value of β_0 corresponding to a maximum value $T_0 = 1/\beta_0$ such that

$$\varphi_0 = \ln(4/e) = \mathcal{H} 2\pi m_{\text{in}}^2 \frac{K_1(\beta_0 m_{\text{in}})}{\beta_0 m_{\text{in}}}. \tag{12.29}$$

This implies, because of Eq. (12.28), that the physical branch of $G(\varphi)$ behaves like

$$G(\beta \simeq \beta_0) = G_0 - \text{constant} \times \sqrt{\beta - \beta_0} \tag{12.30}$$

near β_0.

However, $G(\varphi)$, Eq. (12.23), can have a singularity at β_0 only if

$$\rho(m^2) \to cm^k e^{\beta_0 m}, \qquad m \to \infty. \tag{12.31}$$

The behavior of $G(\beta)$ can be made more explicit by introducing $1 = \int \delta_0(p^2 - m^2) dm^2$ in Eq. (12.23) followed by a change of the sequence of integrals,

$$G = \mathcal{H} \int \rho(m^2) 2\pi m^2 \frac{K_1(\beta m)}{\beta m} dm^2. \tag{12.32}$$

Combining Eq. (12.31) with Eq. (12.32) we find that, for $\beta \to \beta_0$,

$$G(\beta \simeq \beta_0) \approx G_0 + \text{constant} \times \int_{m_{in}}^{\infty} e^{-m(\beta - \beta_0)}\, m^{3/2+k}\, dm, \tag{12.33}$$

which yields

$$G(\beta \to \beta_0) \approx G(\beta_0) + \text{constant} \times \left(\frac{1}{\beta - \beta_0}\right)^{k+5/2} \Gamma(k + \tfrac{5}{2},\, (\beta - \beta_0) m_{\text{in}})\,, \quad (12.34)$$

where Γ is the incomplete gamma function. To obtain a square-root singularity in Eq. (12.34), consistent with Eq. (12.30), one needs $k = -3$.

In summary, the statistical-bootstrap approach assumes that hadrons are clusters consisting of hadrons and that, for large mass, the compound hadrons have the same mass spectrum as that of the constituent hadrons, which leads to a hadronic mass spectrum of the asymptotic form

$$\rho(m^2) \propto m^{-3} e^{m/T_0}. \quad (12.35)$$

This spectrum, as we have seen in Fig. 12.1, describes the known part of the experimental hadronic mass spectrum. For point hadrons, this leads to a singularity of the partition function at T_0, which appears, in view of Eq. (12.8), as a limiting temperature, at which infinite energy density is reached, since $k = -3 > -\frac{7}{2}$.

12.3 Hadrons of finite size

In the first presentation of the SBM results and methods, we have considered point-like hadrons in an arbitrary volume V. For a dilute gas, this is a good approximation. However, when we formulated the bootstrap hypothesis, we dealt with a system that has the density of the 'inside' of a hadron. We now generalize this approach and introduce the volume of the constituent cluster in the spirit of the quark model of hadrons, and confinement; see section 13.1. In the following we will also allow for clusters of finite baryon number.

The natural volume $V(m)$ of a hadron cluster is to be proportional to the cluster mass,

$$V(m) = \frac{m}{4\mathcal{B}}, \quad (12.36)$$

where $\mathcal{B}$, which has the dimension of energy density, is the bag constant; see Eq. (13.9). This equation is valid in the restframe of the cluster. For a cluster with 4-momentum p^μ, Eq. (12.36) takes the form

$$V^\mu(m) = \frac{p^\mu}{4\mathcal{B}}, \quad (12.37)$$

which defines the proper 4-volume V^μ of the particle. In the cluster restframe, Eq. (12.37) reduces to Eq. (12.36) and therefore is its unique generalization. Each object of 4-momentum p_i can be given a volume

https://doi.org/10.1017/9781009290753.017 Published online by Cambridge University Press

V_i^μ. All clusters have the same proper energy density $\epsilon_0 = 4\mathcal{B}$. In a relativistically covariant formulation, we also consider the energy, and the inverse temperature in terms of 4-vectors [261]:

$$E \to p^\mu = (p^0, \vec{p})\,; \qquad p_\mu p^\mu = p\cdot p = m^2, \tag{12.38}$$

$$\frac{1}{T} \to \beta^\mu = (\beta^0, \vec{\beta})\,; \qquad \beta_\mu \beta^\mu = \beta\cdot\beta = \beta^2 = \frac{1}{T^2}. \tag{12.39}$$

Note that the four-dimensional vector product $p \cdot p = (p^0)^2 - (\vec{p})^2$ is recognized by the absence of the vector arrow. In this notation,

$$Z(V,T) = \int_0^\infty \sigma e^{-E/T}\, dE \to \int_0^\infty \sigma e^{-\beta\cdot p} d^4p. \tag{12.40}$$

We now need to obtain the covariant form of the N-finite-sized-particle level density $\sigma_N(p,V,b)$ Eq. (12.10). These particles occupy 'available 4-volume'

$$\Delta^\mu = V^\mu - \sum_{i=1}^{N} V_i^\mu. \tag{12.41}$$

Δ is the volume in which the particles move as if they were point-like, while in reality they have finite proper volumes and move in V. The level density of extended particles in the volume V must be identical to that of the point-like particles in the available volume Δ. This means that, for a system with baryon number b and 4-momentum p,

$$\sigma_N(p,V,b) \equiv \sigma_{N\mathrm{pt}}(p,\Delta,b), \tag{12.42}$$

where 'pt' refers to point-like particles. Equation (12.42) is, in spirit, a Van der Waals correction, which introduces a new repulsive interaction into the system of hadronic resonances.

The generalization to an invariant phase-space volume is

$$\frac{V\, d^3p}{(2\pi)^3} \Rightarrow \frac{2V_\mu p^\mu}{(2\pi)^3}\delta_0(p^2 - m^2)\, d^4p. \tag{12.43}$$

To go back from the invariant form to the restframe we need

$$\delta_0(p^2 - m^2)\, d^4p = \frac{d^3p}{2p_0}. \tag{12.44}$$

Then, in the restframe of the volume V, Eq. (8.17),

$$\boxed{\frac{2V_\mu p^\mu}{(2\pi)^3}\delta_0(p^2 - m^2)\, d^4p = 2Vp_0\frac{d^3p}{2p_0} = \frac{V}{(2\pi)^3}\, d^3p.} \tag{12.45}$$

https://doi.org/10.1017/9781009290753.017 Published online by Cambridge University Press

Therefore, in the Boltzmann approximation, and assigning to each cluster the degeneracy $g \to \tau(m_i^2, b_i)dm_i^2$ with intrinsic baryon content b_i, Eq. (12.10) generalizes to [143]

$$\sigma_N(p,V,b) = \frac{1}{N!}\int \delta^4\!\left(p - \sum_{i=1}^{N} p_i\right)\delta_{\mathrm{K}}\!\left(b - \sum_{i=1}^{N} b_i\right) \times \prod_{i=1}^{N} \frac{2\Delta\cdot p_i}{(2\pi)^3}\tau(m_i^2, b_i)\delta_0(p_i^2 - m_i^2)\, d^4p_i\, dm_i^2. \tag{12.46}$$

$\tau(m_i^2, b_i)$ is the mass spectrum of a cluster with baryon number b_i in the mass interval $[m_i^2, dm_i^2]$. It is the analog of $\rho(m_i^2)$ in Eq. (12.20). The discreet conservation of baryon number is assured by the Kronecker-δ_{K} function.

The micro-canonical Lorentz-invariant density of states of a system made of any number of clusters, each cluster having any baryon number b_i, with $-\infty < b_i < \infty$, reads

$$\boxed{\sigma(p,V,b) = \sum_{N=1}^{\infty}\frac{1}{N!}\int \delta^4\!\left(p - \sum_{i=1}^{N} p_i\right)\sum_{\{b_i\}}\delta_{\mathrm{K}}\!\left(b - \sum_{i=1}^{N} b_i\right) \times \prod_{i=1}^{N} \frac{2\Delta\cdot p_i}{(2\pi)^3}\tau(m_i^2, b_i)\delta_0(p_i^2 - m_i^2)\, d^4p_i\, dm_i^2.} \tag{12.47}$$

In Eq. (12.47), the contributing states are subdivided into any number of subsets corresponding to any partition of the total 4-momentum p^μ and the total baryon number b.

The canonical partition function, for a fixed baryon number b, is the Laplace transform of the level density given by Eq. (12.47),

$$Z(T,V,b) = \int e^{-\beta\cdot p}\, d^4p \sum_{N=1}^{\infty}\frac{1}{N!}\int \delta^4\!\left(p - \sum_{i=1}^{N} p_i\right)\sum_{\{b_i\}}\delta_{\mathrm{K}}\!\left(b - \sum_{i=1}^{N} b_i\right) \times \prod_{i=1}^{N} \frac{2\Delta\cdot p_i}{(2\pi)^3}\tau(m_i^2, b_i)\delta_0(p_i^2 - m_i^2)\, d^4p_i\, dm_i^2, \tag{12.48}$$

from which we obtain the grand-canonical partition function, Eq. (4.20), defined by

$$\mathcal{Z}(T,V,\lambda) = \sum_{\mathrm{b}} \lambda^b Z(T,V,b) = \sum_{b=-\infty}^{\infty}\lambda^b \int e^{-\beta\cdot p}\sigma(p,V,b)\, d^4p, \tag{12.49}$$

where λ is the baryon-number fugacity corresponding to the baryonic chemical potential μ: $\lambda = \exp \mu/T$.

https://doi.org/10.1017/9781009290753.017 Published online by Cambridge University Press

To implement Eq. (12.42), we postulate

$$\mathcal{Z}(T, V, \lambda) \to \mathcal{Z}(T, \langle V \rangle, \lambda) = \mathcal{Z}_{\rm pt}(T, \Delta, \lambda). \tag{12.50}$$

Equation (12.50) permits us to calculate everything for fictitious point particles in Δ and afterwards obtain the correct quantities by eliminating Δ in favor of a computed, average value $\langle V \rangle$. Use of $\langle V \rangle$ instead of V constitutes an approximation, and a lot of effort over the years, since this approach was first proposed [143], has gone into remedying this step in a consistent statistical-physics approach, and into generalizing the idea contained in Eq. (12.42). A state-of-the-art calculation is given, e.g., in [170]. However, the original and physically simple model presented here offers all the required understanding without the ballast of mathematical complexity, and yields sufficiently precise results.

$\mathcal{Z}_{\rm pt}(T, \Delta, \lambda)$ can be written in the form

$$\begin{aligned}\mathcal{Z}_{\rm pt}(T, \Delta, \lambda) = &\sum_{N=1}^{\infty} \frac{1}{N!} \int \delta^4\!\left(p - \sum_{i=1}^{N} p_i\right) e^{-\beta \cdot p}\, d^4p \\ &\times \sum_{b=-\infty}^{\infty} \lambda^b \sum_{\{b_i\}} \delta_{\rm K}\!\left(b - \sum_{i=1}^{N} b_i\right) \prod_{i=1}^{N} \frac{2\Delta \cdot p_i}{(2\pi)^3} \tau(p_i^2, b_i)\, d^4p_i.\end{aligned} \tag{12.51}$$

The momentum δ^4 function permits us to do the d^4p integration and the $\delta_{\rm K}$ permits the summation over b. The integrand thereafter splits into N independent identical integrals, and the sum over N yields an exponential function. Taking its logarithm, we obtain

$$\ln \mathcal{Z}_{\rm pt}(T, \Delta, \lambda) \equiv \ln \mathcal{Z}(T, \langle V \rangle, \lambda) = \mathcal{Z}_1(T, \Delta, \lambda), \tag{12.52}$$

where

$$\mathcal{Z}_1(T, \Delta, \lambda) \equiv \int \frac{2\Delta \cdot p}{(2\pi)^3} \tau(p^2, \lambda) e^{-\beta \cdot p}\, d^4p, \tag{12.53}$$

with

$$\tau(p^2, \lambda) = \sum_{b=-\infty}^{\infty} \lambda^b \tau(p^2, b). \tag{12.54}$$

All information about the interaction is contained in the ‘grand-canonical’ hadronic mass spectrum $\tau(m^2, \lambda)$.

We obtain now the relation between $\langle V \rangle$ and Δ in the restframe. We use Eq. (12.37) to find the expectation value of the volume:

$$\langle V^\mu \rangle = \Delta^\mu + \frac{p^\mu}{4\mathcal{B}} \to \Delta + \left.\frac{\langle E \rangle}{4\mathcal{B}}\right|_{\rm restframe}. \tag{12.55}$$

The energy density $\epsilon(\beta,\lambda)$ can be obtained from Eq. (12.52), for the energy:

$$\langle E\rangle = -\frac{\partial}{\partial\beta}\ln\mathcal{Z}(\beta,\langle V\rangle,\lambda) = -\frac{\partial}{\partial\beta}\ln\mathcal{Z}_{\rm pt}(\beta,\Delta,\lambda). \tag{12.56}$$

Since $\ln\mathcal{Z}_{\rm pt}$ is linear in Δ, the last term is equal to $\Delta\epsilon_{\rm pt}(\beta,\lambda)$; hence,

$$\epsilon(\beta,\lambda) = \frac{\Delta\epsilon_{\rm pt}(\beta,\lambda)}{\langle V\rangle}. \tag{12.57}$$

Inserting Eq. (12.55) into Eq. (12.57) and solving for $\langle E\rangle$, we find

$$\boxed{\epsilon(\beta,\lambda) = \frac{\epsilon_{\rm pt}(\beta,\lambda)}{1+\epsilon_{\rm pt}(\beta,\lambda)/(4\mathcal{B})},} \tag{12.58}$$

which we have used in Eq. (11.1).

We can use Eq. (12.58) in Eq. (12.55) to obtain a more explicit relationship between the volume V and the available volume Δ:

$$\langle V\rangle = \Delta\left(1+\frac{\epsilon_{\rm pt}(\beta,\lambda)}{4\mathcal{B}}\right), \tag{12.59a}$$

$$\Delta = \langle V\rangle\left(1-\frac{\epsilon(\beta,\lambda)}{4\mathcal{B}}\right). \tag{12.59b}$$

This procedure can be followed for the baryon density, pressure and, in principle, other statistical quantities:

$$\boxed{\nu(\beta,\lambda) \equiv \frac{\langle b\rangle}{\langle V\rangle} = \frac{\nu_{\rm pt}(\beta,\lambda)}{1+\epsilon_{\rm pt}(\beta,\lambda)/(4\mathcal{B})},} \tag{12.60}$$

$$\boxed{P(\beta,\lambda) = \frac{P_{\rm pt}(\beta,\lambda)}{1+\epsilon_{\rm pt}(\beta,\lambda)/(4\mathcal{B})}.} \tag{12.61}$$

12.4 Bootstrap with hadrons of finite size and baryon number

As explained in section 12.2 a system of total mass m, when it is compressed to its natural volume $V_{\rm c}(m)$, becomes one of the particles counted in the hadronic mass spectrum (see Fig. 12.4). By the same token, a nuclear cluster with baryon number b compressed to its natural volume $V_{\rm c}(m,b)$ becomes a cluster appearing in the mass spectrum $\tau(m^2,b)$. The bootstrap hypothesis can now be expressed by writing

$$\sigma(p,\Delta,b)|_{\langle v\rangle\to v_c(m,b)} \Longleftrightarrow \tau(p^2,b), \tag{12.62}$$

https://doi.org/10.1017/9781009290753.017 Published online by Cambridge University Press

where $\Longleftrightarrow$ means 'corresponds to' in a way to be specified.

With the condition Eq. (12.62), the statistical-bootstrap-model equation for τ arises from Eq. (12.47):

$$\boxed{\begin{aligned}\mathcal{H}\tau(p^2,b) = \mathcal{H}g_{\rm b}\delta_0(p^2-m_{\rm b}^2) + \sum_{N=2}^{\infty}\frac{1}{N!}\int\delta^4\!\left(p-\sum_{i=1}^{N}p_i\right)\\ \times\sum_{\{b_i\}}\delta_{\rm K}\!\left(b-\sum_{i=1}^{N}b_i\right)\prod_{i=1}^{N}\mathcal{H}\tau(p_i^2,b_i)\,d^4p_i,\end{aligned}} \tag{12.63}$$

where

$$\mathcal{H} \equiv \frac{2m_0^2}{(2\pi)^3 4\mathcal{B}}. \tag{12.64}$$

This equation is obtained, by first separating the 'input particle' (corresponding to $N = 1$) in Eq. (12.47), and then making the following replacement, where Eq. (12.37) is used:

$$\sigma(p, V_c, b) \Rightarrow \frac{2V_c(m,b)\cdot p}{(2\pi)^3}\tau(p^2,b) \Rightarrow \frac{2m_0^2}{(2\pi)^3 4\mathcal{B}}\tau(p^2,b), \tag{12.65a}$$

$$\frac{2\Delta\cdot p_i}{(2\pi)^3}\tau(p_i^2,b_i) \Rightarrow \frac{2m_0^2}{(2\pi)^3 4\mathcal{B}}\tau(p_i^2,b_i). \tag{12.65b}$$

The factors m^2 and m_i^2 have been absorbed into the definition of $\tau(p_i^2, b_i)$. Either $\mathcal{H}$ or m_0 may be taken as the new free parameter of the model.

The first term in Eq. (12.63), the 'input-particle' term, comes from the cluster structure: if clusters consist of clusters, which consist of clusters, and so on, this should end at some 'elementary' particles, here a hadron of baryon number b and of mass $m_{\rm b}$. Typically, the input consists of the pion for the $b = 0$ term and the nucleon for $b = \pm 1$. The similarity of Eq. (12.63) to Eq. (12.20) allows us to repeat all the steps we made in solving Eq. (12.20), to obtain from Eq. (12.63) the asymptotic form of the hadronic mass spectrum. We introduce two functions $\varphi(\beta, \lambda)$ and Φ:

$$\begin{aligned}\varphi(\beta,\lambda) &\equiv \int e^{-\beta\cdot p}\sum_{b=-\infty}^{\infty}\lambda^b\mathcal{H}g_{\rm b}\delta_0(p^2-m_{\rm b}^2)\,d^4p,\\ &= 2\pi\mathcal{H}\sum_{b=-\infty}^{\infty}\lambda^b g_{\rm b}m_{\rm b}^2\frac{K_1(m_{\rm b}\beta)}{m_{\rm b}\beta},\end{aligned} \tag{12.66}$$

and

$$\Phi(\beta,\lambda) \equiv \int e^{-\beta\cdot p}\sum_{b=-\infty}^{\infty}\lambda^b\mathcal{H}\tau(p^2,b)\,d^4p. \tag{12.67}$$

Once the set of 'input particles' is introduced, $\varphi(\beta,\lambda)$ is a known function, while $\Phi(\beta,\lambda)$ is unknown. By applying the double Laplace transform (integration over p and summation over b) used in the definition of $\varphi(\beta,\lambda)$ and $\Phi(\beta,\lambda)$ to the Eq. (12.63), we obtain

$$\Phi(\beta,\lambda)=\varphi(\beta,\lambda)+e^{\Phi(\beta,\lambda)}-\Phi(\beta,\lambda)-1. \tag{12.68}$$

This implicit equation for Φ can be solved again without regard to the actual dependence on β and λ. Writing

$$G(\varphi)\equiv\Phi(\beta,\lambda), \tag{12.69}$$

we obtain

$$\varphi=2G(\varphi)-\exp[G(\varphi)]+1, \tag{12.70}$$

which is Eq. (12.25). The graphical solution found in section 12.2 shows that $G(\varphi,\lambda)$ has a square-root singularity at

$$\varphi(\beta,\lambda)\to\varphi_0=\ln(4/e), \tag{12.71}$$

which defines a critical curve $\beta_{\rm cr}(\lambda)$ in the $(\beta,\,\lambda)$ plane. In the vicinity of this curve,

$$G(\varphi)\approx G_0+\text{constant}\times\sqrt{\varphi_0-\varphi}, \tag{12.72}$$

and, therefore,

$$\Phi(\lambda,\beta\simeq\beta_{\rm cr})=\Phi_0-C(\lambda)\sqrt{\beta-\beta_{\rm cr}}. \tag{12.73}$$

As we have shown in section 12.2, this square-root singularity fixes the power k of m in the hadronic mass spectrum at $k=-3$ and we obtain

$$\tau(m^2,\lambda)\propto m^{-3}e^{\beta_{\rm cr}(\lambda)m}. \tag{12.74}$$

For $\lambda=1$, $\beta_{\rm cr}=\beta_0$ and we recover the usual form of the hadronic mass spectrum. However, the generalization obtained gives a solution for any value of λ.

Given the mass spectrum in Eq. (12.52), we can calculate all the usual thermodynamic quantities. For this, we need to write down $\ln\mathcal{Z}_{\rm pt}$. The formal similarity of Eq. (12.53) and Eq. (12.67) yields a relation between $\ln\mathcal{Z}_{\rm pt}$ and Φ that is best expressed in the restframe of Δ and β:

$$\boxed{\ln\mathcal{Z}_{\rm pt}(T,\Delta,\lambda)=-\frac{2\Delta}{(2\pi)^3\mathcal{H}}\frac{\partial}{\partial\beta}\Phi(\beta,\lambda).} \tag{12.75}$$

https://doi.org/10.1017/9781009290753.017 Published online by Cambridge University Press

The point-like quantities are derived from $\ln \mathcal{Z}_{\rm pt}$ as given by Eq. (12.75):

$$\epsilon_{\rm pt}(\beta,\lambda) = \frac{2}{(2\pi)^3\mathcal{H}}\frac{\partial^2}{\partial\beta^2}\Phi(\beta,\lambda), \tag{12.76}$$

$$\nu_{\rm pt}(\beta,\lambda) \equiv \frac{\lambda}{\Delta}\frac{\partial}{\partial\lambda}\ln \mathcal{Z}_{\rm pt}(\beta,\Delta,\lambda) = -\frac{2\lambda}{(2\pi)^3\mathcal{H}}\frac{\partial}{\partial\lambda}\frac{\partial}{\partial\beta}\Phi(\beta,\lambda), \tag{12.77}$$

$$P_{\rm pt}(\beta,\lambda) \equiv \frac{T}{\Delta}\ln \mathcal{Z}_{\rm pt}(\beta,\Delta,\lambda) = -\frac{2T}{(2\pi)^3\mathcal{H}}\frac{\partial}{\partial\beta}\Phi(\beta,\lambda). \tag{12.78}$$

All the above point-particle quantities involve derivatives of $\Phi(\beta,\lambda)$; they become singular at $\varphi = \varphi_0$. Explicitly, using Eq. (12.72), which contains a square-root singularity, we have:

$$\frac{\partial}{\partial\beta}\Phi(\beta,\lambda) = \frac{dG}{d\varphi}\frac{\partial\varphi}{\partial\beta} \to \text{constant} \times \frac{\partial\varphi}{\partial\beta}\frac{1}{\sqrt{\varphi_0-\varphi}}. \tag{12.79}$$

Therefore, $\varphi \to \varphi_0$ implies point-particle infinities for all of the above quantities, with the second derivative required in $\epsilon_{\rm pt}$ being the most singular. On comparing the degrees of divergence of the numerator and denominator in Eqs. (12.58), (12.60), and (12.61), we see that the energy density and the baryon density are finite, while the pressure vanishes, on the critical curve. The overcompensation of the pressure is seen already in Fig. 12.3, which was evaluated with a model hadron mass spectrum.

This behavior of the pressure reflects the fact that we have counted only the pressure generated by the clusters and, as we shall see in the following subsection, all clusters coalesce on the critical curve, and hence the pressure of a single large cluster vanishes. This of course is an artifact, since at that point we should have included the internal cluster pressure, since the single cluster we find is in the QGP-type state. We will not introduce in this book the required generalization which can be found in [213].

12.5 The phase boundary in the SBM model

We have seen that the singular point of the solution to the bootstrap equation is located at the value $\varphi_0 = \ln(4/e)$ and that the critical curve in the $(\beta,\,\lambda)$ plane is defined by

$$\varphi(\beta,\lambda) = \varphi_0 = \ln(4/e). \tag{12.80}$$

Its position depends, of course, on the actual content of $\varphi(\beta,\lambda)$, i.e., on the fundamental set of 'elementary particles' $\{m_{\rm b},\ g_{\rm b}\}$ and the value of the constant $\mathcal{H}$, Eq. (12.64). In the case of three elementary pions $(\pi^+\pi^0\pi^-)$

https://doi.org/10.1017/9781009290753.017 Published online by Cambridge University Press

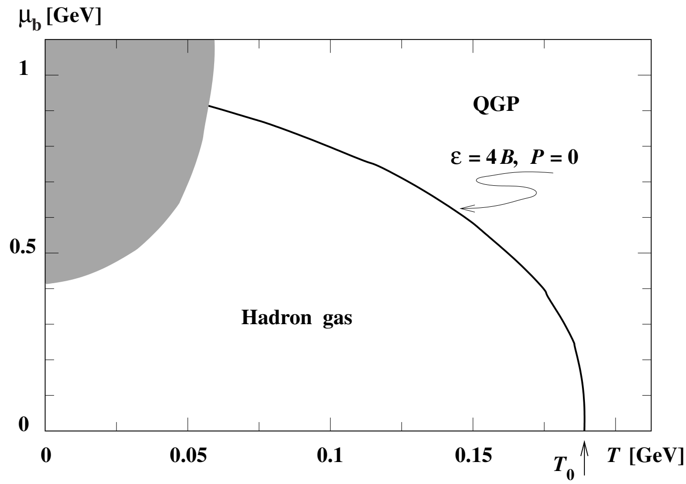

Fig. 12.6. The SBM critical curve in the ($\mu_{\rm b}$, T) plane. In the shaded region, the theory is not valid because we have neglected Bose–Einstein and Fermi–Dirac statistics.

and four elementary nucleons (spin ⊗ isospin) and four antinucleons, we obtain, from Eq. (12.66), the relation

$$\varphi_0(\beta_{\rm cr},\lambda_{\rm cr}) = 2\pi\mathcal{H}T_{\rm cr}\left[3m_\pi K_1\left(\frac{m_\pi}{T_{\rm cr}}\right) + 4\left(\lambda_{\rm cr}+\frac{1}{\lambda_{\rm cr}}\right)m_{\rm N}K_1\left(\frac{m_{\rm N}}{T_{\rm cr}}\right)\right]. \tag{12.81}$$

The condition of Eq. (12.81), written in $T_{\rm cr} = 1/\beta_{\rm cr}$ and $\mu_{\rm cr} = T_{\rm cr}\ln\lambda_{\rm cr}$, yields the critical curve shown in Fig. 12.6, drawn for $\mathcal{H} = 0.724$ GeV^{-2}. For $\mu = 0$, the curve ends at $T = T_0$, which becomes the maximum phase transition temperature instead of a limiting temperature.

Our system consists, for small T and μ, of nucleons and nuclei. For increasing T, creation of pions sets in and finally also creation of baryon–antibaryon pairs, as well as (not included here) creation of strange hadrons. If the latter is taken into account, the input set of 'elementary particles' has to be enlarged. This changes slightly the position of the critical curve and the equations of state of hadron matter, since T_0 is of the order of the pion mass, while the other particles have larger masses and make little contribution to $\varphi(\beta,\lambda)$. More precisely, each new conserved quantum number (strangeness, charm, ...) gives rise to another corresponding fugacity λ; hence the singularity is defined by $\varphi(\beta,\lambda_1,\lambda_2,\lambda_3,\ \ldots,\lambda_n) = \varphi_0$ as a hypersurface in an $(n+1)$-dimensional space. Since, however, in physical situations, generally only the baryon number is different from zero, we have to consider only the intersection of this hypersurface with the $(T,\, \mu_{\rm b})$ plane. That procedure yields the curve which was said to be little different from the one shown in Fig. 12.6.

What does the SBM hadron gas do when it approaches the critical curve? As the point-particle quantities $\epsilon_{\rm pt}$, $\nu_{\rm pt}$, and $p_{\rm pt}$ diverge, one sees (by comparing degrees of divergence when $\varphi \to \varphi_0$) that

$$\epsilon(\beta_{\rm cr}, \lambda_{\rm cr}) \to 4\mathcal{B}, \tag{12.82a}$$
$$\nu(\beta_{\rm cr}, \lambda_{\rm cr}) \to \nu_{\rm cr}(\beta_{\rm cr}, \lambda_{\rm cr}) \neq 0, \tag{12.82b}$$
$$P(\beta_{\rm cr}, \lambda_{\rm cr}) \to 0, \tag{12.82c}$$
$$\Delta(\beta_{\rm cr}, \lambda_{\rm cr}) \to 0, \qquad \text{if } \langle V\rangle \neq 0, \tag{12.82d}$$
$$\langle V(\beta_{\rm cr}, \lambda_{\rm cr})\rangle \to \infty, \qquad \text{if } \quad \Delta \neq 0, \tag{12.82e}$$

where $\beta_{\rm cr}$ and $\lambda_{\rm cr}$ are the values along the critical curve.

As noted already, see Eq. (12.36), the energy density of our clusters was constant and always equal to $4\mathcal{B}$. Equation (12.82a) suggests that, on the critical curve, the whole hadron system has condensed into one giant cluster, witnessed by the vanishing of the pressure; one can explicitly see that, for any given external volume $\langle V\rangle$, the number $\langle N\rangle$ of particles (clusters) contained in it goes to zero on the critical curve: indeed, introducing the fugacity ξ relative to the number of clusters, Eq. (12.52) can be written:

$$\mathcal{Z}_{\rm pt}(\beta, \Delta, \lambda) = \mathcal{Z}^{(\xi)}_{\rm pt}(\beta, \Delta, \lambda, \xi)|_{\xi=1} \equiv \sum_{N=0}^{\infty} \frac{1}{N!}(\xi \, \ln \mathcal{Z}_{\rm pt})^N. \tag{12.83}$$

Hence, with Eq. (12.75),

$$\langle N\rangle = \xi \frac{\partial}{\partial \xi} \ln \mathcal{Z}^{(\xi)}_{\rm pt}\bigg|_{\xi=1} = \ln \mathcal{Z}_{\rm pt} = -\frac{2\Delta}{(2\pi)^3 \mathcal{H}} \frac{\partial}{\partial \beta}\Phi(\beta, \lambda), \tag{12.84}$$

and, with Eq. (12.59a),

$$\frac{\langle N\rangle}{\langle V\rangle} = \frac{\mathcal{B}}{\pi^3 \mathcal{H}} \frac{\partial \Phi(\beta, \lambda)/\partial \beta}{1 + \epsilon_{\rm pt}(\beta, \lambda)} \underset{\text{critical curve}}{\Longrightarrow} 0, \tag{12.85}$$

because $\epsilon_{\rm pt}$ contains a second derivative of $\Phi(\beta, \lambda)$. It follows that, from Eqs. (12.61), (12.78), and (12.85),

$$P\langle V\rangle = \langle N\rangle T, \tag{12.86}$$

that is, our hadron gas obeys, formally, the ideal-gas equation of state for the average number of clusters $\langle N\rangle$; $\langle N\rangle$ is not a constant, but a function of β and λ.

In the bootstrap model of hadronic gas, our finding is that the critical curve limits the HG phase; approaching it, all hadrons dissolve into a giant

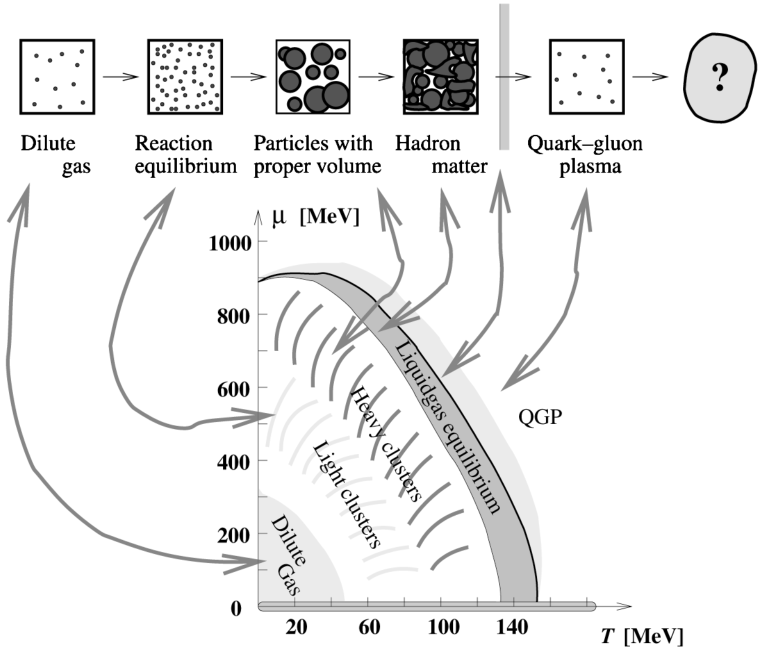

Fig. 12.7. The physical interpretation of the different regions of the $(T,\ \mu)$ plane according to the statistical-bootstrap model of hadronic matter.

cluster. The gradual change in the structure of hot hadronic matter is illustrated in Fig. 12.7; at low T, μ we have a dilute pion gas of essentially point-like pions. With an increase in T and/or μ, progressively denser hadron matter is formed, and hadron proper volume becomes relevant. Near the phase boundary hadrons coalesce into large clusters comprising drops of QGP.

In SBM the singular curve is reached with finite energy density $4\mathcal{B}$. In the hadron phase, $\epsilon(\beta, \lambda) < 4\mathcal{B}$ and $\beta \leq \beta_{\rm cr}$. For $\epsilon > 4\mathcal{B}$, we enter into a region that cannot be described by the thermodynamics of the SBM. Indeed in this region, $\beta \geq \beta_{\rm cr}$ and the partition function $\mathcal{Z}_{\rm pt}(\beta, \Delta, \lambda)$ and all densities become complex. This region cannot be described without making assumptions about the inner structure and dynamics of the 'elementary particles' $\{m_{\rm b},\ g_{\rm b}\}$ – here pions and nucleons – entering into the input function $\varphi(\beta, \lambda)$. In other words, to continue, we need to consider the hot hadron interior made of quarks and gluons. Assuming that we have a phase transition between a HG and a QGP, the evolution of the system in the P–V diagram is qualitatively illustrated in Fig. 3.2 on page 49. In order to make this picture quantitative we need to explore, within the realm of quantum chromodynamics, the hadron structure and the behavior of a gas of quarks and gluons with color interactions.